

A Graphical and Semi-Quantitative Technique for Investigating Vertical Electrical Sounding (VES) Curves for Indices of Confined Fractured Basement Column.

Adebayo O. Ojo, M.Sc.^{1*} and Martins O. Olorunfemi, Ph.D.²

¹Department of Geosciences, University of Lagos, Akoka, Lagos, Nigeria.

²Department of Geology, Obafemi Awolowo University, Ile-Ife, Nigeria.

E-mail: ojo.adebayo.oluwaseun@gmail.com*

ABSTRACT

Although, the mathematical analysis for the quantitative interpretation of resistivity data is most highly developed for the Vertical Electrical Sounding (VES) technique adopting the Schlumberger array, the modeling and interpretation of VES curve is inextricably linked with the principle of equivalence and suppression, which makes it inherently non-unique. A typical geological situation in which suppression could be encountered is in a basement complex profile involving a fractured column sandwiched between an upper and bottom fresh basement columns commonly referred to as confined fractured basement. Delineation of such confined fractured column on the VES curve through the conventional method of visual inspection can be highly subjective. In an attempt to resolve this detectability problem, an improved identification technique involving the numerical computation of the first and second derivative of the apparent resistivity dataset has been developed. The efficacy of the newly developed technique is tested on both synthetic and field observed VES dataset.

(Keywords: VES, confined fractured basement, semi-quantitative interpretation)

INTRODUCTION

Identifying a good site for groundwater development in water scarce basement complex terrain is a challenging task. In hard rock terrain, groundwater occurs in media with secondary porosity (developed due to weathering, fracturing, faulting, etc.), which are highly variable and vary sharply within very short distances, contributing to near-surface inhomogeneity. In a typical basement complex environment, fractured basement columns have been identified as a very

important lithological unit which contributes significantly to the productiveness and yields of boreholes (Olayinka and Oladipo, 1994). However, to image this important hydrogeological unit in the subsurface, the Vertical Electrical Sounding (VES) technique of the electrical resistivity method utilizing the Schlumberger electrode configuration has been highly favoured because of its field logistic advantages in addition to the fact that it yields useful information about the subsurface condition (Sheriff, 1992; Olorunfemi and Fasuyi, 1993; Patra and Nath, 1999).

The first step in the conventional method of interpretation of Schlumberger VES dataset involves the plotting of the measured apparent resistivity values (in ohm-meter) against half the spread length or electrode spacing (in meter) on a log-log graph sheet to obtain a sounding curve. The sounding curve is then interpreted using the partial curve matching technique which involves segment by segment matching of the VES curve with two layer model master curves and associated auxiliary curves to obtain the layer parameters (i.e., the layer resistivity and thicknesses).

At this stage of interpretation, the number of segment fitted to the VES curve is a function of the number of layers that can be visually identified by the interpreter. This is highly subjective as it depends on the interpreter's experience and expertise especially in a geologically complex environment. However, a layer whose resistivity is intermediate between that of the enclosing layers without appreciable thickness will be suppressed. Such layer will not reflect on the VES curve and will automatically be missed out of interpretation consideration. This generally leads to misinterpretation of the VES curve. A typical geological unit that is susceptible

to being suppressed is a confined fractured basement column (which is a potentially good aquiferous layer in the subsurface) sandwiched between two fresh basement columns in areas underlain by crystalline basement rocks (Olorunfemi and Faluyi, 1993; Olayinka and Oladipo, 1994; Ademilua and Olorunfemi, 2010).

Example of a multilayered earth model containing a confined fractured basement column typical in a basement complex terrain is shown in Figure 1.

For a five-layer earth model (Figure 1) with resistivity combination $\rho_1 > \rho_2 < \rho_3 > \rho_4 < \rho_5$, when the confined fractured basement column and the overlying and underlying fresh basement layers are detectable on the VES curve, a typical resistivity depth sounding HKH-type curve which

is obviously segmented and displaced along the rising basements segment is observed (Figure 2).

In this case, the whole curve is correctly interpreted as a five-layer HKH-type curve. However, when the confined fractured basement is suppressed the resultant VES curve is not segmented and displaced, the VES curve can be erroneously viewed/interpreted as either a four-layer HA type curve or a three-layer H-type curve as the case may be. Figure 3 presents superimposed VES curves resulting from two different five-layer geologic models. The figure illustrates a situation where a five-layer geologic model containing a confined fractured basement column resulted into a three-layer VES curve. This is a classic case of suppression which this study is aimed to address.

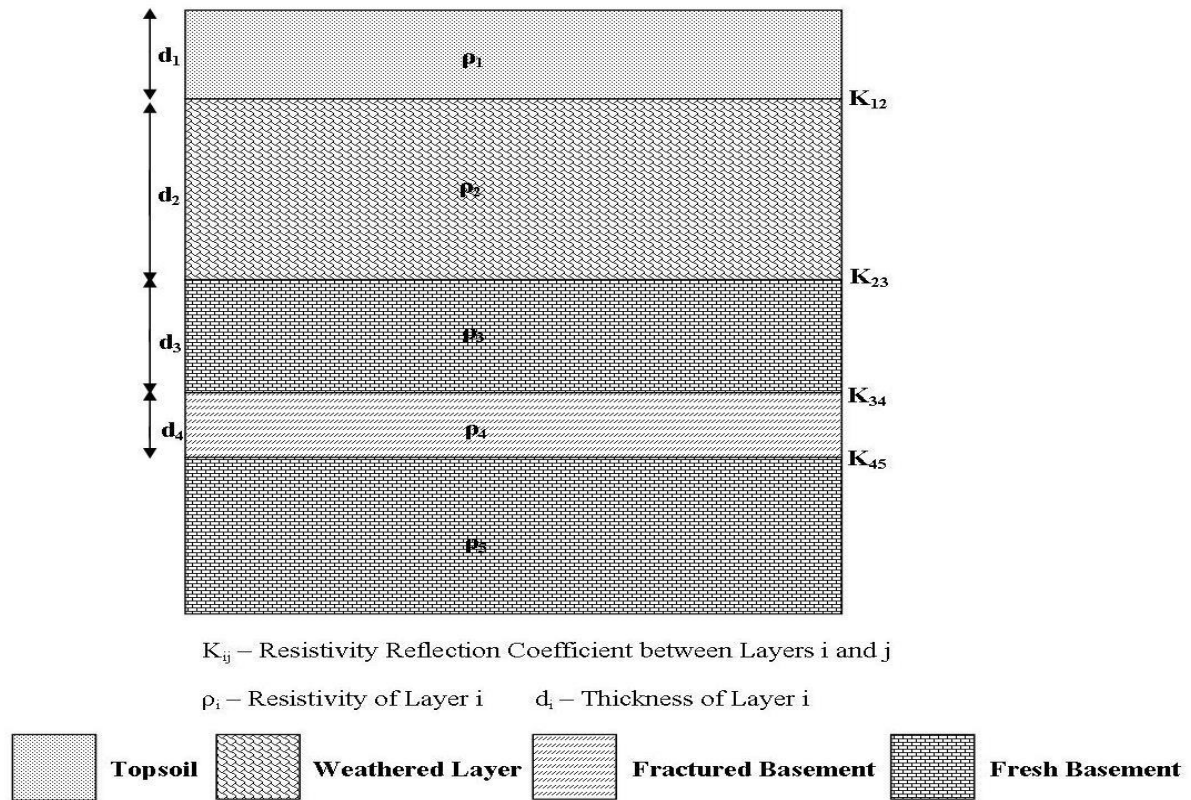
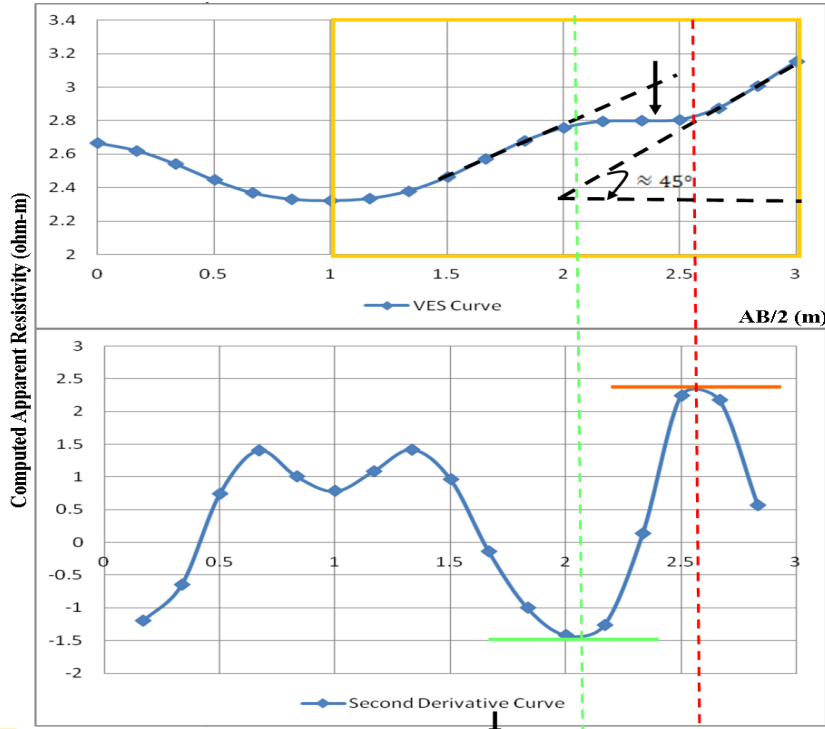


Figure 1: A Typical Five-Layer Earth Model Containing a Confined Fractured Basement Column in a Basement Complex Terrain.



 Rising Segment of VES Curve Typifying the Basement
 Inflection
 Inflection Trough
 Inflection Peak

Note: This chart is plotted in logarithm. The actual value to be obtained is 10 raised to the power of the value read on this chart.

Figure 2: Geoelectric Signature of a Typical Basement Profile Containing a Confined Fractured Basement Column in a Basement Complex Terrain.

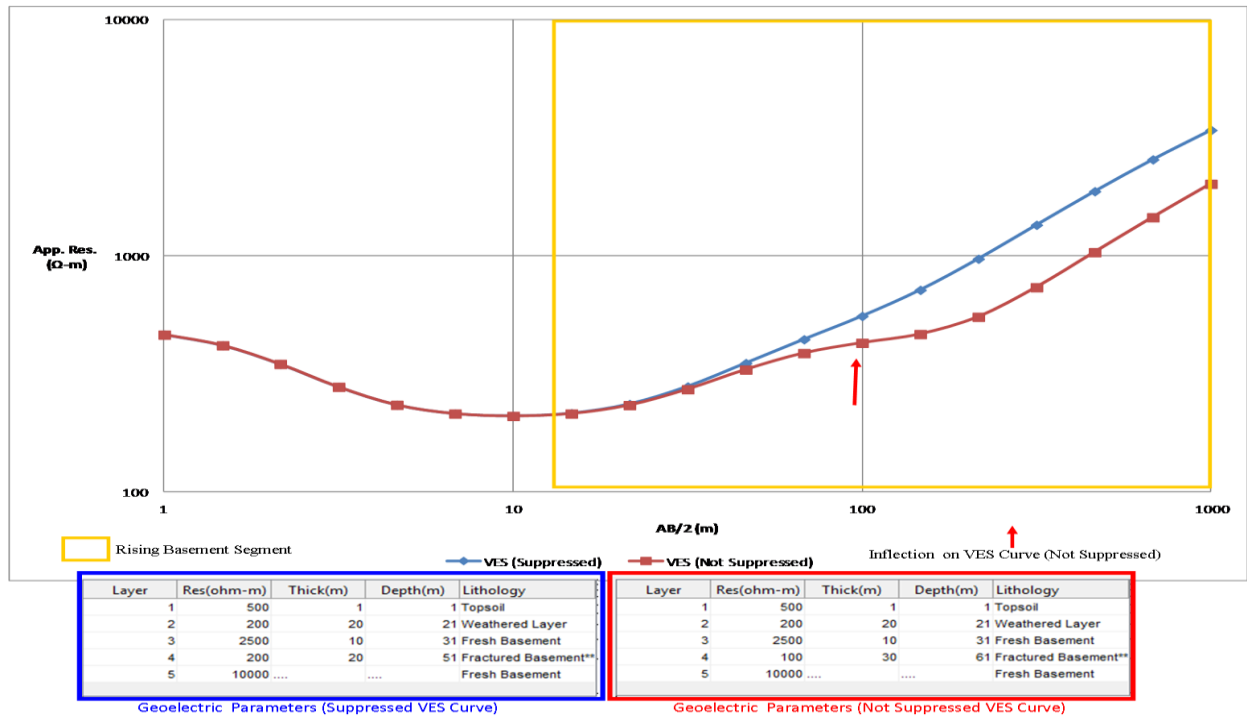


Figure 3: Superimposed VES Curves of Two Five-layer Geologic Models Containing a Confined Fractured Basement Column.

METHODOLOGY

A forward modeling computer software (SyntheticVES) developed by the authors (Ojo and Olorunfemi, 2013) for generating theoretical Schlumberger Vertical Electrical Sounding (VES) curves was used to compute theoretical apparent resistivity dataset for series of five-layer geologic models (Figure 1) containing a confined fractured basement column with varying geoelectric parameters.

The logarithms of the generated VES dataset from the different multilayered earth models (i.e. apparent resistivity values for specific electrode spacing (AB/2) values) were first computed. Subsequently, the second derivative of the resistivity dataset was then computed from the logarithm VES dataset numerically using Equation 1 recurrently (twice) to compute the second derivative of the theoretical apparent resistivity dataset and their respective electrode spacing values using Equation 2.

$$(Res)_i = \frac{((Res)_{i+1} - (Res)_i)}{\left(\left(\frac{AB}{2}\right)_{i+1} - \left(\frac{AB}{2}\right)_i\right)} \quad (1)$$

$$\left(\frac{AB}{2}\right)_i = \left(\frac{AB}{2}\right)_{i+1} + \frac{\left(\left(\frac{AB}{2}\right)_{i+1} - \left(\frac{AB}{2}\right)_i\right)}{2} \quad (2)$$

where $(Res)_i$ is the apparent resistivity value of data point i ; $\left(\frac{AB}{2}\right)_i$ is the electrode spacing value for data point i ; $(Res)_{i+1}$ is the apparent resistivity value of the next data point $i+1$ and $\left(\frac{AB}{2}\right)_{i+1}$ is the electrode spacing value for the next data point $i+1$.

A superposed plot of the VES curves, and the second derivative curve was made and the segment of the VES curve corresponding to the rising basement segments on the derivative curves was then analyzed for indices of the confined fractured basement column. Conventionally, a confined fractured basement column is imaged as an inflection along the rising segments of the VES curve (Olorunfemi and Fasuyi, 1993) (see also Figure 2). While the fresh basement columns display VES curve segments that rise to up to 45° with respect to the horizontal axis and are somewhat parallel. As shown in Figure 2, the beginning of the inflection on the VES curve which characterizes the

confined fractured column coincides with the trough of the second derivative curve while the peak corresponds to the end of the inflection. There is a coincidence in the inflections for both the VES and the second derivative curves.

To determine if the newly developed technique has any form of advantage over the conventional method of visual inspection, in resolving a confined basement fracture, the generated VES curves from different geologic models A, B and C (Figure 4) and their respective geoelectric parameters display in Tables 1 - 3 were subjected to visual inspection aided by fitting parallel inclined ($\approx 45^\circ$) lines to the rising segments of the VES curves at large electrode spacing and check if an inflection typical of the confined fractured basement columns was identifiable between the two fitted lines while simultaneously checking if an inflection is also observed along the second derivative curve of the VES dataset.

Table 1: Geologic Model and Geoelectric Parameter for Model A.

Layer	Res(ohm-m)	Thick(m)	Depth(m)	Lithology
1	500	1		1 Topsoil
2	200	20		21 Weathered Layer
3	2500	40		61 Fresh Basement
4	100	20		81 Fractured Basement*
5	10000	Fresh Basement

Table 2: Geologic Model and Geoelectric Parameter for Model B.

Layer	Res(ohm-m)	Thick(m)	Depth(m)	Lithology
1	500	1		1 Topsoil
2	200	20		21 Weathered Layer
3	2500	10		31 Fresh Basement
4	100	10		41 Fractured Basement**
5	10000	Fresh Basement

Table 3: Geologic Model and Geoelectric Parameter for Model C.

Layer	Res(ohm-m)	Thick(m)	Depth(m)	Lithology
1	500	1		1 Topsoil
2	200	20		21 Weathered Layer
3	2500	40		61 Fresh Basement
4	400	20		81 Fractured Basement**
5	10000	Fresh Basement

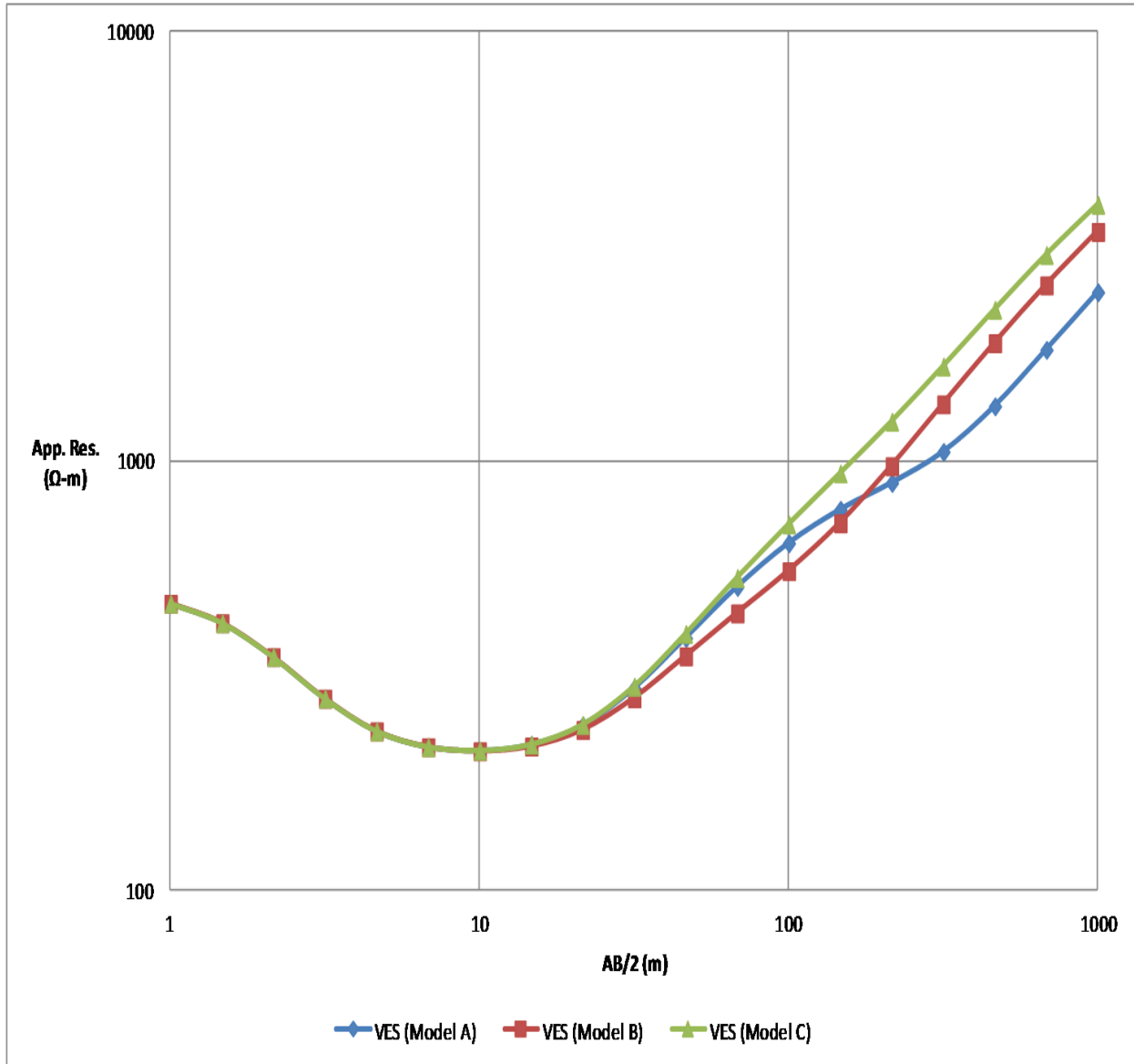


Figure 4: Superimposed VES Curves Generated for Geologic Models A, B and C.

RESULTS AND DISCUSSION

The computed VES dataset using the SyntheticVES software, the logarithm of the VES dataset, the first and second derivative of the

VES dataset are presented in Tables 4 - 6 and a superposed plot of the VES curve and the second derivative curve are presented in Figures 5 - 7.

Table 4: Computed Dataset for Geologic Model A.

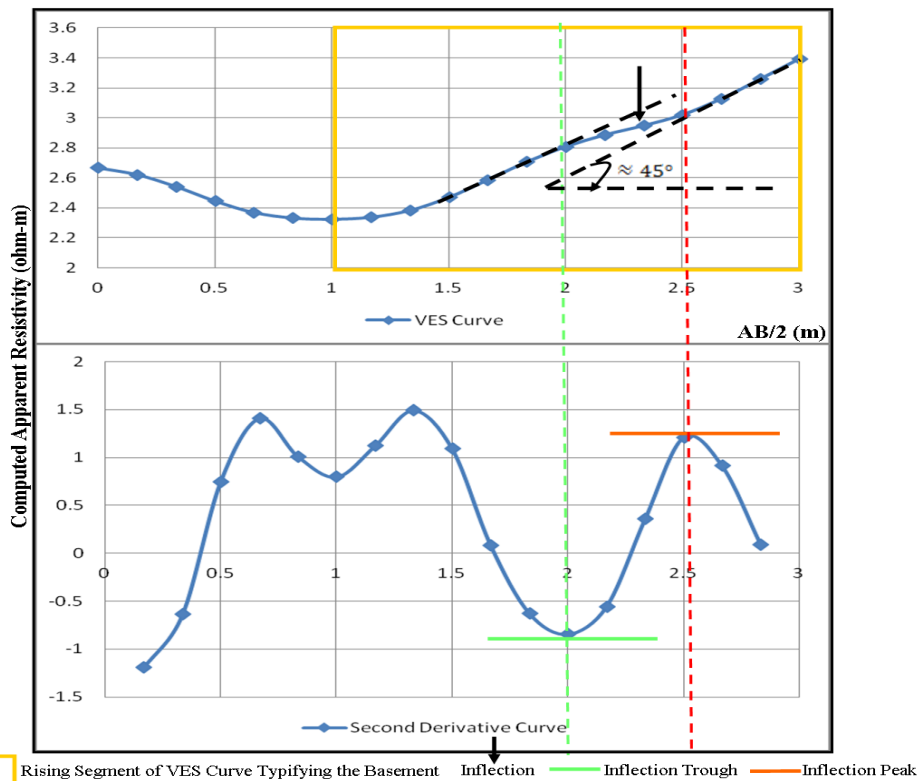
DATASET A Computed Dataset		DATASET B Converted Data to Logarithm Scale		DATASET C First Derivative Dataset (Applying Equation 1 & 2 on Dataset B)		DATASET D Second Derivative Dataset (Applying Equation 1 & 2 on Dataset C)	
AB/2 (m)	Comp. Res. (Ohm-m)	LOG10 (AB/2) (m)	LOG10 (Comp. Res.) (Ohm-m)	LOG10(AB/2) (m)	LOG10(Comp. Res.) (Ohm-m)	LOG10(AB/2) (m)	LOG10(Comp. Res.) (Ohm-m)
1	464.36	0	2.6669	0.0837	-0.2716	0.1673	-1.1957
1.47	418.23	0.1673	2.6214	0.2510	-0.4716	0.3346	-0.6418
2.15	348.74	0.3324	2.5425	0.4161	-0.5790	0.4998	0.7434
3.16	279.01	0.4997	2.4456	0.5833	-0.4546	0.6670	1.4046
4.64	234.18	0.6665	2.3695	0.7502	-0.2196	0.8338	1.0076
6.81	215.18	0.8331	2.3328	0.9168	-0.0510	1.0005	0.7936
10	210.99	1.0000	2.3243	1.0837	0.0817	1.1673	1.1181
14.68	217.74	1.1667	2.3379	1.2504	0.2688	1.3340	1.4881
21.54	241.5	1.3332	2.3829	1.4169	0.5178	1.5006	1.0884
31.62	294.82	1.5000	2.4696	1.5836	0.6999	1.6673	0.0801
46.42	386.07	1.6667	2.5867	1.7504	0.7133	1.8340	-0.6279
68.13	508.18	1.8333	2.7060	1.9170	0.6083	2.0007	-0.8452
100	642.38	2.0000	2.8078	2.0837	0.4668	2.1673	-0.5584
146.78	768.96	2.1667	2.8859	2.2503	0.3734	2.3340	0.3544
215.44	887.94	2.3333	2.9484	2.4170	0.4327	2.5006	1.2069
316.23	1049.02	2.5000	3.0208	2.5837	0.6347	2.6673	0.9098
464.16	1339.59	2.6667	3.1270	2.7503	0.7869	2.8340	0.0907
681.29	1813.97	2.8333	3.2586	2.9170	0.8021	-	-
1000	2470.75	3.0000	3.3928	-	-	-	-

Table 5: Computed Dataset for Geologic Model B.

DATASET A Computed Dataset		DATASET B Converted Data to Logarithm Scale		DATASET C First Derivative Dataset (Applying Equation 1 & 2 on Dataset B)		DATASET D Second Derivative Dataset (Applying Equation 1 & 2 on Dataset C)	
AB/2 (m)	Comp. Res. (Ohm-m)	LOG10 (AB/2) (m)	LOG10 (Comp. Res.) (Ohm-m)	LOG10(AB/2) (m)	LOG10(Comp. Res.) (Ohm-m)	LOG10(AB/2) (m)	LOG10(Comp. Res.) (Ohm-m)
1	464.36	0.00	2.67	0.08	-0.27	0.17	-1.20
1.47	418.23	0.17	2.62	0.25	-0.47	0.33	-0.64
2.15	348.74	0.33	2.54	0.42	-0.58	0.50	0.74
3.16	278.99	0.50	2.45	0.58	-0.46	0.67	1.40
4.64	234.1	0.67	2.37	0.75	-0.22	0.83	0.98
6.81	214.93	0.83	2.33	0.92	-0.06	1.00	0.72
10	210.23	1.00	2.32	1.08	0.06	1.17	0.95
14.68	215.45	1.17	2.33	1.25	0.22	1.33	1.20
21.54	234.78	1.33	2.37	1.42	0.42	1.50	0.74
31.62	276.37	1.50	2.44	1.58	0.55	1.67	-0.13
46.42	341.32	1.67	2.53	1.75	0.53	1.83	-0.33
68.13	417.89	1.83	2.62	1.92	0.47	2.00	0.36
100	500.84	2.00	2.70	2.08	0.53	2.17	1.06
146.78	614.21	2.17	2.79	2.25	0.71	2.33	0.83
215.44	806.55	2.33	2.91	2.42	0.85	2.50	0.14
316.23	1117.09	2.50	3.05	2.58	0.87	2.67	-0.20
464.16	1561.46	2.67	3.19	2.75	0.84	2.83	-0.32
681.29	2154.12	2.83	3.33	2.92	0.78	-	-
1000	2911.15	3.00	3.46	-	-	-	-

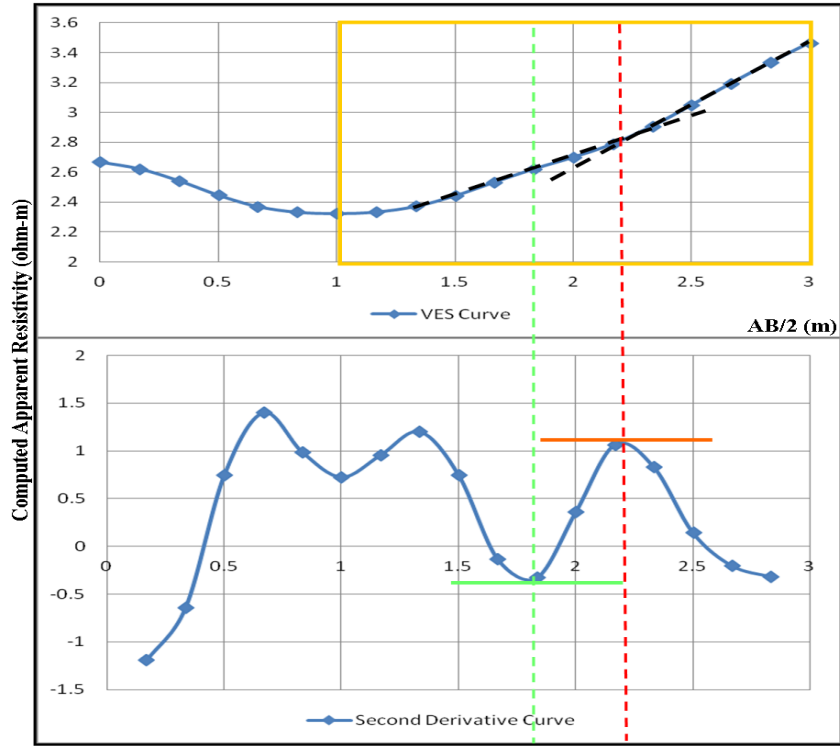
Table 6: Computed Dataset for Geologic Model C.

DATASET A Computed Dataset		DATASET B Converted Data to Logarithm Scale		DATASET C First Derivative Dataset (Applying Equation 1 & 2 on Dataset B)		DATASET D Second Derivative Dataset (Applying Equation 1 & 2 on Dataset C)	
AB/2 (m)	Comp. Res. (Ohm-m)	LOG10 (AB/2) (m)	LOG10 (Comp. Res.) (Ohm-m)	LOG10(AB/2) (m)	LOG10(Comp. Res.) (Ohm-m)	LOG10(AB/2) (m)	LOG10(Comp. Res.) (Ohm-m)
1	464.36	0.00	2.67	0.08	-0.27	0.17	-1.20
1.47	418.23	0.17	2.62	0.25	-0.47	0.33	-0.64
2.15	348.74	0.33	2.54	0.42	-0.58	0.50	0.74
3.16	279.01	0.50	2.45	0.58	-0.45	0.67	1.41
4.64	234.18	0.67	2.37	0.75	-0.22	0.83	1.01
6.81	215.19	0.83	2.33	0.92	-0.05	1.00	0.80
10	211.06	1.00	2.32	1.08	0.08	1.17	1.14
14.68	218.01	1.17	2.34	1.25	0.28	1.33	1.54
21.54	242.4	1.33	2.38	1.42	0.53	1.50	1.19
31.62	297.65	1.50	2.47	1.58	0.73	1.67	0.29
46.42	394.7	1.67	2.60	1.75	0.78	1.83	-0.22
68.13	533.34	1.83	2.73	1.92	0.74	2.00	-0.20
100	710.57	2.00	2.85	2.08	0.71	2.17	0.07
146.78	934.45	2.17	2.97	2.25	0.72	2.33	0.27
215.44	1234.31	2.33	3.09	2.42	0.77	2.50	0.14
316.23	1659.01	2.50	3.22	2.58	0.79	2.67	-0.17
464.16	2249.68	2.67	3.35	2.75	0.76	2.83	-0.37
681.29	3018.12	2.83	3.48	2.92	0.70	-	-
1000	3952.65	3.00	3.60	-	-	-	-



Note: This chart is plotted in logarithm. The actual value to be obtained is 10 raised to the power of the value read on this chart.

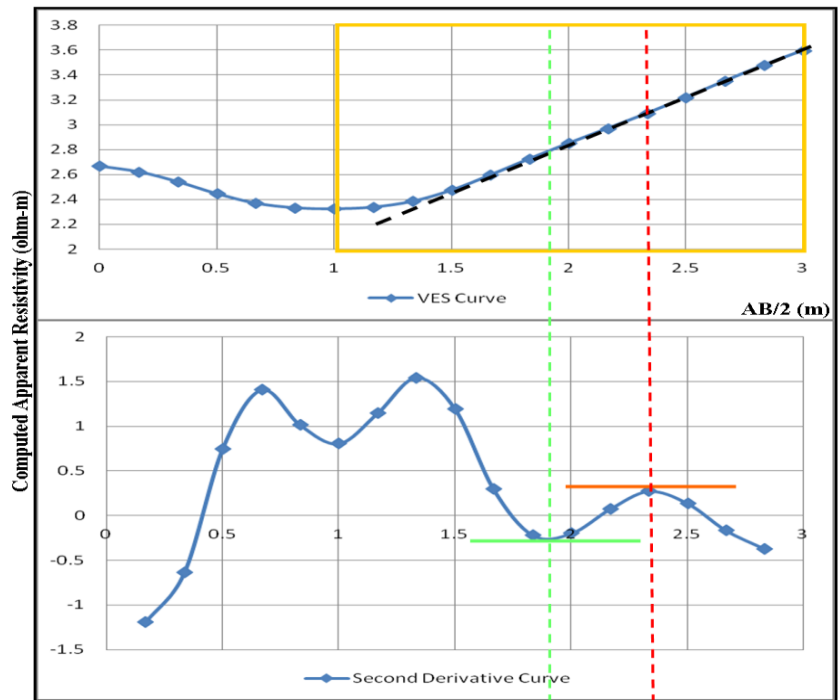
Figure 5: Superposed Curve of VES data and Second Derivative of the VES data for Model A.



 Rising Segment of VES Curve Typifying the Basement
 — Inflection Trough
 — Inflection Peak

Note: This chart is plotted in logarithm. The actual value to be obtained is 10 raised to the power of the value read on this chart.

Figure 6: Superposed Curve of VES data and Second Derivative of the VES data for Model B.



 Rising Segment of VES Curve Typifying the Basement
 — Inflection Trough
 — Inflection Peak

Note: This chart is plotted in logarithm. The actual value to be obtained is 10 raised to the power of the value read on this chart.

Figure 7: Superposed Curve of VES data and Second Derivative of the VES data for Model C.

For model A, the geoelectric parameters are presented in Table 1, the computed VES dataset using the Synthetic VES software, the logarithm of the VES dataset, the first and second derivative of the VES dataset are presented in Table 4 and a superposed plot of the VES curve and the second derivative curve are presented in Figure 4. Using the visual inspection method aided by fitting parallel inclined $\approx 45^\circ$ lines to the rising segments of the VES curve as denoted by a box in Figure 5, it can be observed that the inflection (denoted by an arrow on Figure 5) characterizing the presence of the confined fractured basement column is easily identifiable on the VES curve. This is a case where the confined fractured basement column is not suppressed and the VES curve displays the HKH-type curve. The inflection on the VES curve typifying the confined fractured basement coincides with an inflection on the second derivative curve whose trough coincides with the beginning of the inflection on the VES curve while its peak coincides with the end of the inflection. This makes the position of the inflection characterizing the presence of the confined fractured basement column on the VES curve easily identifiable on the second derivative curve as also marked out by the two dotted vertical lines in Figure 5.

Model B is a case where a five-layer geologic model containing a confined fractured basement column is modelled and the theoretically computed VES dataset was plotted but the inflection characterizing the presence of the confined fractured basement column is not visually discernible on the VES curve due to geoelectric suppression of the layer. The geoelectric parameters of this model are presented in Table 2, the computed VES dataset using the Synthetic VES software, the logarithm of the VES dataset, the first and second derivative of the VES dataset are presented in Table 5 and a superposed plot of the VES curve and the second derivative curve are presented in Figure 6. By fitting parallel inclined $\approx 45^\circ$ lines to the rising basement segments of the VES curve as denoted by a box in Figure 6, it is observed that the VES curve is only segmented but not displaced (indicating an inflection), hence, the inflection characterizing the presence of the confined fractured basement column is not identifiable on the VES curve. A five-layer geologic model which is expected to display an HKH-type depth sounding curve display a four-

layer HA-type VES curve due to suppression of the confined fractured basement column. Therefore, from the visual inspection method alone, this curve would be basically interpreted as a four layer HA-type curve. However, the second derivative curve imaged the supposed position of the inflection on the VES curve whose limits are defined by the trough and peak of the second derivative curve (see Figure 6) on the rising segment of the VES curve. This position is also marked out by two dotted vertical lines in Figure 6.

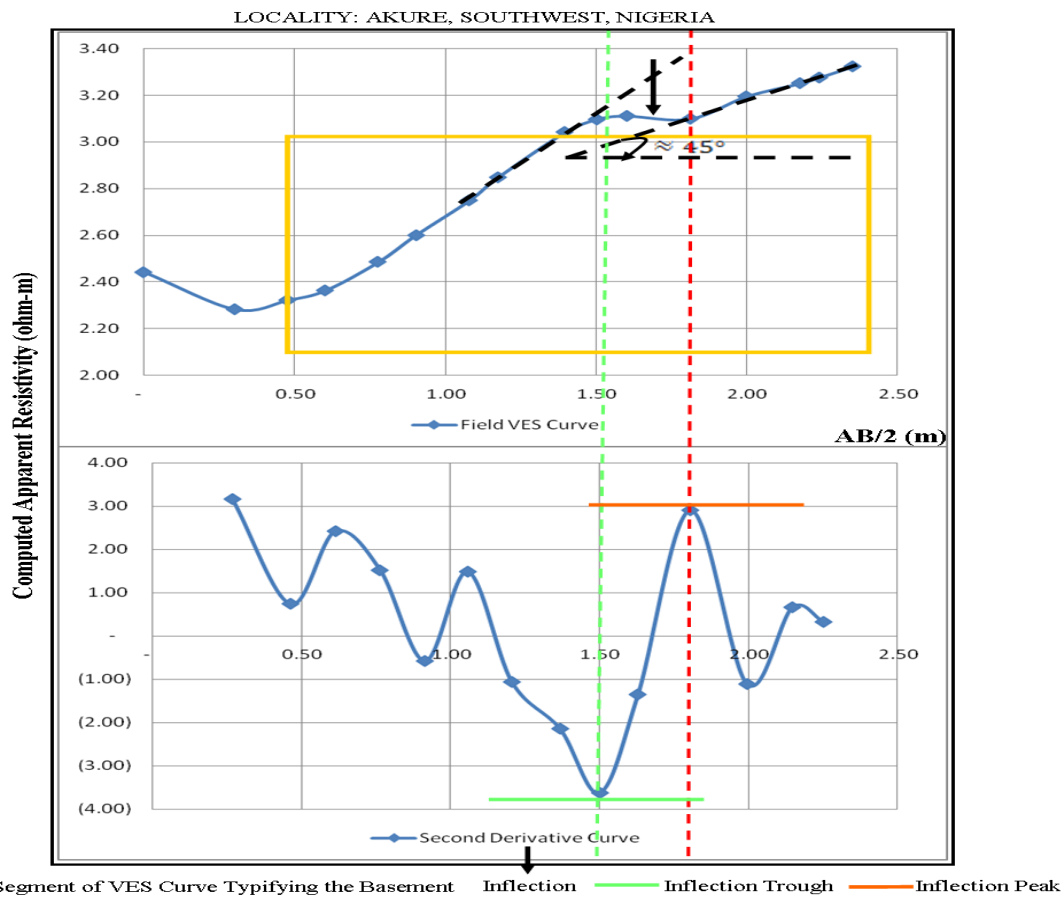
Model C is a five-layer geologic model containing a confined fractured basement column in which the theoretically computed VES dataset are plotted but the inflection characterizing the presence of the confined fractured basement column is not identifiable on the VES curve due to suppression. The geoelectric parameters of this model are presented in Table 3. The computed theoretical VES dataset using the Synthetic VES software, the logarithm of the VES dataset, the first and second derivative of the VES dataset are computed and presented in Table 6. The superposed plot of the VES curve and the second derivative curve are presented in Figure 7. This is another case where the confined fractured basement column is suppressed on the VES as can be clearly observed from the visual inspection of the VES curve in Figure 7. Fitting a parallel inclined $\approx 45^\circ$ line to the rising basement segment of the VES curve within the box in Figure 7, shows that the VES curve is neither segmented nor displaced; hence, the inflection characterizing the presence of the confined fractured basement column on the VES curve is not identifiable. In this case, a five-layer geologic model which is expected to display an HKH-type depth sounding curve now manifest as a three-layer H-type VES curve due to suppression of the confined fractured basement column. The confined fractured basement column has been merged with the two basement segments and the three different layers have been imaged as a single layer. Therefore, using the conventional visual inspection method, this curve would be basically interpreted as a three layer curve. However, the second derivative curve imaged the supposed position of the inflection on the VES curve whose limits are defined by the trough and peak of the second derivative curve (see Figure 7) on the rising segment of the VES curve. This position is also marked out by two dotted vertical lines in Figure 4.

Field Example

To illustrate the efficacy of the newly developed technique on field VES data, four VES dataset acquired from Ile-Ife and Akure, Southwest, Nigeria and interpreted to contain confined fractured basement column was utilized. The interpreted geoelectric model, the field VES curve and the second derivative curve of each of the field example are presented in Figures 8 to 11.

As has been previously observed on the synthetic VES examples, the inflection (denoted by an arrow on Figures 8 – 11) characterizing the

presence of the confined fractured basement column on the field VES curve and its position was imaged on the second derivative curve. This is denoted by an inflection whose trough coincides with the beginning of the inflection typifying the confined fractured basement on the field VES curves while its peak also coincides with the end of the inflection thereby marking the position of the fractured basement column. The field examples showed that the newly developed technique can serve as an alternative way to cross check if a field VES curve contains a confined fractured basement column as illustrated in Figures 8, 9 and 10.



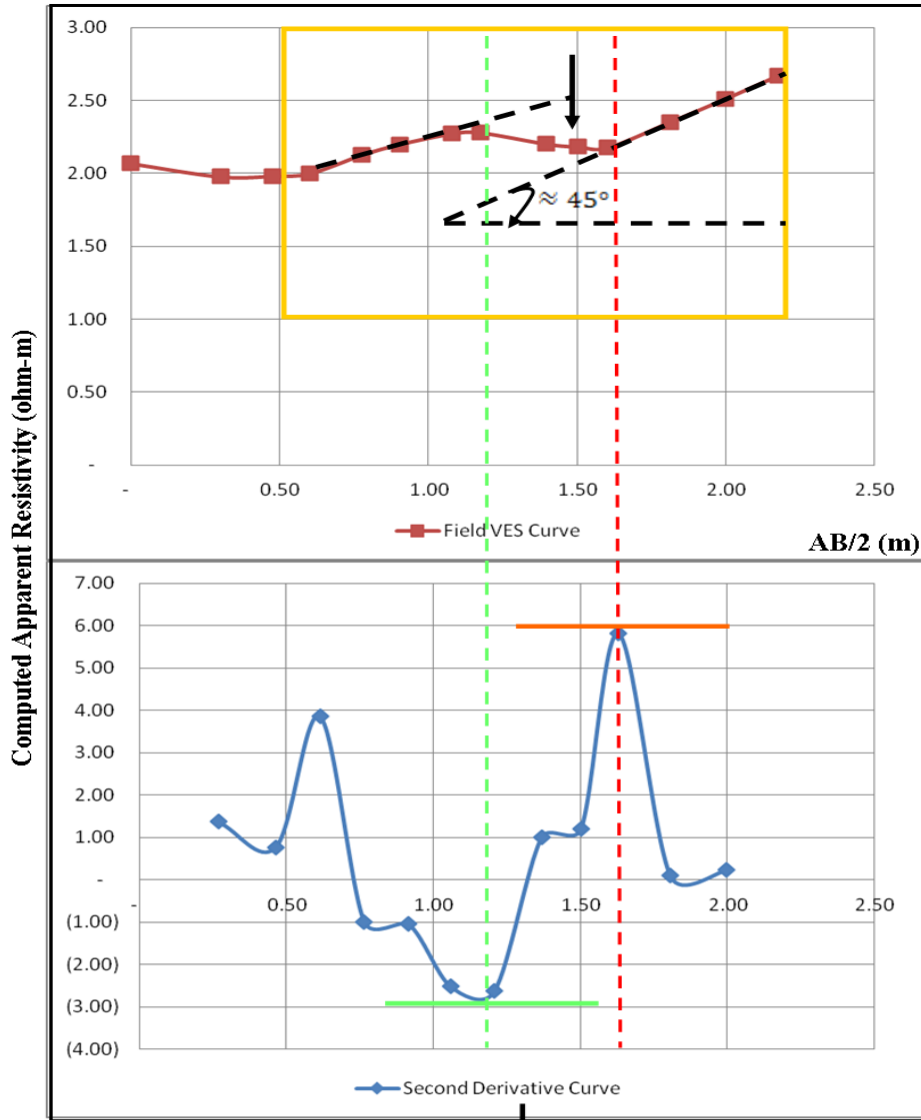
Note: This chart is plotted in logarithm. The actual value to be obtained is 10 raised to the power of the value read on this chart.

INTERPRETED GEOELECTRIC MODEL

Layer	Res(ohm-m)	Thick(m)	Depth(m)	Lithology
1	506	0.3800	0.3800	Topsoil
2	157	2.7000	3.0800	Weathered Layer
3	4528	16	19.0800	Fresh Basement
4	159	12	31.0800	Fractured Basement
5	99999	Fresh Basement

Figure 8: Field Example One Showing Field VES Curve and Second Derivative Curve and Interpreted Geoelectric Model.

LOCALITY: ILE-IFE, SOUTHWEST, NIGERIA



 Rising Segment of VES Curve Typifying the Basement
 Inflection
 Inflection Trough
 Inflection Peak

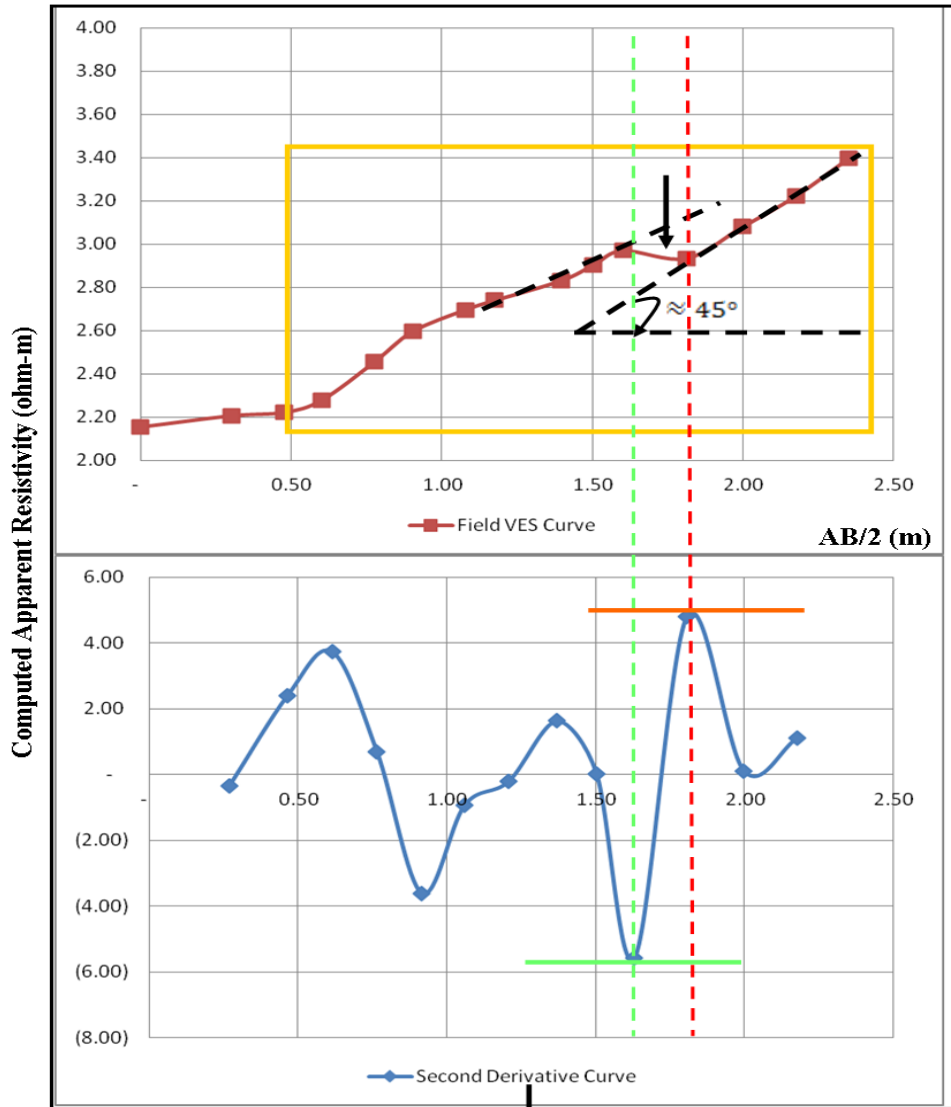
Note: This chart is plotted in logarithm. The actual value to be obtained is 10 raised to the power of the value read on this chart.

INTERPRETED GEOELECTRIC MODEL

Layer	Res(ohm-m)	Thick(m)	Depth(m)	Lithology
1	174	0.4200	0.4200	Topsoil
2	72	2.2000	2.6200	Weathered Layer
3	814	2.1000	4.7200	Fresh Basement
4	81	22	26.7200	Fractured Basement
5	100000	Fresh Basement

Figure 9: Field Example Two Showing Field VES Curve and Second Derivative Curve and Interpreted Geoelectric Model.

LOCALITY: AKURE, SOUTHWEST, NIGERIA



 Rising Segment of VES Curve Typifying the Basement
 Inflection
— Inflection Trough
— Inflection Peak

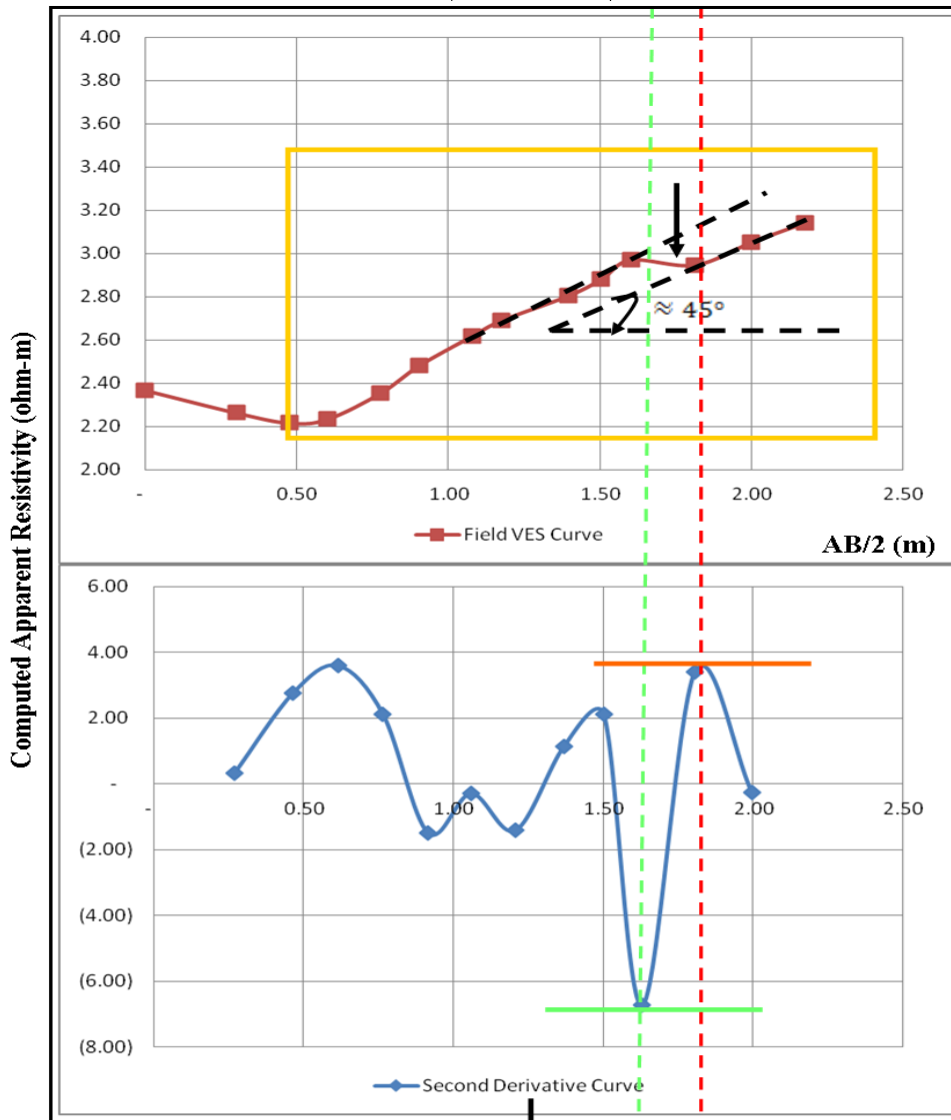
Note: This chart is plotted in logarithm. The actual value to be obtained is 10 raised to the power of the value read on this chart.

INTERPRETED GEOELECTRIC MODEL

Layer	Res(ohm-m)	Thick(m)	Depth(m)	Lithology
1	138	2.4000	2.4000	Topsoil
2	1422	18	20.4000	Fresh Basement
3	509	30	50.4000	Fractured Basement
4	99999	Fresh Basement

Figure 10: Field Example Three Showing Field VES Curve and Second Derivative Curve and Interpreted Geoelectric Model.

LOCALITY: AKURE, SOUTHWEST, NIGERIA



 Rising Segment of VES Curve Typifying the Basement
 Inflection
 Inflection Trough
 Inflection Peak

Note: This chart is plotted in logarithm. The actual value to be obtained is 10 raised to the power of the value read on this chart.

INTERPRETED GEOELECTRIC MODEL

Layer	Res(ohm-m)	Thick(m)	Depth(m)	Lithology
1	268	0.7700	0.7700	Topsoil
2	106	2.2000	2.9700	Weathered Layer
3	1911	23	25.9700	Fresh Basement
4	308	25	50.9700	Fractured Basement
5	99999	Fresh Basement

Figure 11: Field Example Four Showing Field VES Curve and Second Derivative Curve and Interpreted Geoelectric Model.

CONCLUSION

A graphical and semi-quantitative technique for investigating Vertical Electrical Sounding (VES) curves for indices of confined fractured basement column have been developed and the efficacy of the newly developed technique has been tested on synthetic VES dataset generated from some multilayered earth models and field measurements. This newly developed technique can serve as a very useful aid in the interpretation of VES curve most especially in the event of geoelectric suppression of confined basement columns.

REFERENCES

1. Ademilua, L.O. and M.O. Olorunfemi. 2010. "Computer Modeling for Assessing the Detectability of the Transition Zone in the Basement Complex Terrain of Southwest Nigeria". *Pacific Journal of Science and Technology*. 11(2): 674-698.
2. Ojo, A.O. and M.O. Olorunfemi. 2013. "A Graphical User Interface (GUI) MATLAB Program Synthetic_VES for Computation of Theoretical Schlumberger Vertical Electrical Sounding (VES) Curves for Multilayered Earth Models". *Ife Journal of Science*. 15(1):51 – 61.
3. Olayinka, A.I. and A.O. Oladipo. 1994. "A Quantitative Assessment of Geoelectrical Suppression in Four-Layer HA-type Earth Model". *Journal of Mining and Geology*. 30(2):251-258.
4. Olorunfemi, M.O. and A.S. Fasuyi. 1993. "Aquifer Types and the Geoelectric/Hydrogeologic Characteristics of the Basement Terrain of Niger State, Nigeria". *Journal of African Earth Sciences*. 16(3):309-317.
5. Patra, H.P. and S.K. Nath. 1999. *Schlumberger Geoelectric Sounding in Groundwater: Principles, Interpretation and Applications*. Balkema Publishers: Rotterdam. 153 pp.
6. Sherrif, S.D. 1992. "Spreadsheet Modeling of Electrical Sounding Experiments". *Groundwater*. 30(6): 971-974.

ABOUT THE AUTHORS

Adebayo Oluwaseun Ojo, received a Diploma in Computer Technology, a Bachelor of Science (B.Sc.) degree in Engineering Physics, and a Master of Science (M.Sc.) degree in Applied Geophysics, from the Obafemi Awolowo

University, Ile-Ife, Nigeria. He is currently an Assistant Lecturer in the Department of Geosciences of the University of Lagos, Akoka, Lagos, Nigeria and is researching to earn a Ph.D. degree in Applied Geophysics.

Olorunfemi Martins Olusola, is a Professor of Applied Geophysics in the Department of Geology, Obafemi Awolowo University, Ile-Ife. He received his B.Sc., from the University of Ife, Ile-Ife, Nigeria with first class honors, after which he proceeded to the University of Birmingham, U.K., for his M.Sc. and Ph.D., both in Applied Geophysics. He has edited several journals at the local, national, and international levels. He researches in groundwater, environmental, mineral and engineering geophysics.

SUGGESTED CITATION

Ojo, A.O. and M.O. Olorunfemi. 2013. "A Graphical and Semi-Quantitative Technique for Investigating Vertical Electrical Sounding (VES) Curves for Indices of Confined Fractured Basement Column". *Pacific Journal of Science and Technology*. 14(2):537-550.

 [Pacific Journal of Science and Technology](http://www.akamaiuniversity.us/PJST.htm)